XLVI CILAMCE
VITÓRIA - ES - BRAZIL - 2025
XLVI IBERO-LATIN AMERICAN CONGRESS ON COMPUTATIONAL METHODS IN ENGINEERING

Numerical Analysis of Stress Concentration Factors in Mooring Chain Links Tensioned with and without Geometric Barriers

Evilly Raquel H. da Silveira[1], Michele A.L. Martins[1], Eduardo N. Lages[1], Mauro C. Oliveira[2]

[1]*Computing and Visualization Laboratory, Federal University of Alagoas*
Cidade Universitária, 57072-970, Maceió/AL, Brazil
evilly.silveira@ctec.ufal.br, micheleagra@lccv.ufal.br, enl@lccv.ufal.br
[2]*CENPES/PETROBRAS*
Av. Horácio Macedo, 950 - Cidade Universitária da Universidade Federal do Rio de Janeiro, 21941-915, Rio de Janeiro/RJ, Brazil
mauro@petrobras.com.br

Abstract. The increasing demand for energy resources, combined with technological advancements, has enabled the exploration of offshore fields at increasingly greater depths. This scenario imposes more severe environmental conditions, requiring continuous improvement of guidelines and standards for mooring analysis and design. Conversely, there has been a significant increase in the number of mooring line incidents over the years. Despite advancements in understanding the behavior of these systems and their relationship with failure events, some gaps still exist. The interaction between the mooring chain links and devices such as chain hawses, mooring chocks, and fairleads - responsible for guiding or restricting the upper end of mooring lines - is often overlooked, and research in this area is limited. This study investigates the influence of interaction between mooring chain links and geometric barriers on stress concentration factors. A three-dimensional finite element model is developed using Abaqus to simulate chain links under combined tension, bending, and torque. Results show that the presence of geometric barriers significantly alters the behavior of the links and the locations of critical stress points. Furthermore, the interaction between the links and curved surfaces of different radii significantly influenced the accumulated plastic strain of the chain links. The study also examines the impact of residual stress fields from proof load testing, demonstrating that their omission leads to notable differences in the results. These findings highlight the importance of accurately representing the real configuration of mooring chain links in numerical models to support more accurate fatigue assessments under actual operating conditions.

Keywords: Mooring chain links, Geometric barriers, Stress concentration factors, Residual stresses.

1 Introduction

The growing demand for energy resources, combined with technological advancements, has enabled the exploration of offshore fields in environments with increasingly severe conditions, requiring the continuous improvement of guidelines and standards applied to the analysis and design of mooring systems.

Mooring lines are designed for a service life exceeding twenty years of continuous operation. However, failures are reported to occur in a significantly shorter period than the expected design life. Researchers reviewed incidents that occurred between 1997 and 2013 and identified an increasing trend over the years in the number of mooring line failures or preventive replacements [1]. There is a possibility of a future increase in these incidents due to the growth in the number of offshore structures [2].

Bureau Veritas [3], the American Bureau of Shipping [4], and the American Petroleum Institute [5] provide important recommendations for assessing fatigue in mooring chain links; however, certain limitations can still be observed in these guidelines. The finite element modeling proposed for locating critical stress points disregards the possibility that the top section of the mooring line may interact with mooring system accessories [6]. However, mooring lines originate from inside the floating platforms and pass through a guiding device leading to the sea [7].

These devices serve to guide or restrict the movement of the upper end of the line and include equipment such as chain hawsers, mooring chocks, and fairleads. Contact interactions can be identified between the links of the upper segment of the line and these devices [8].

Furthermore, the residual stress state resulting from proof load testing is often omitted when evaluating critical stress points. This aspect can significantly influence the behavior and fatigue life of the chain links [9]. This practice is typically justified by the assumption that, under operational conditions, the chain link responds linearly and plastic strain are not observed. However, this approach may not adequately capture the effective stresses experienced by the chain links during operation [10].

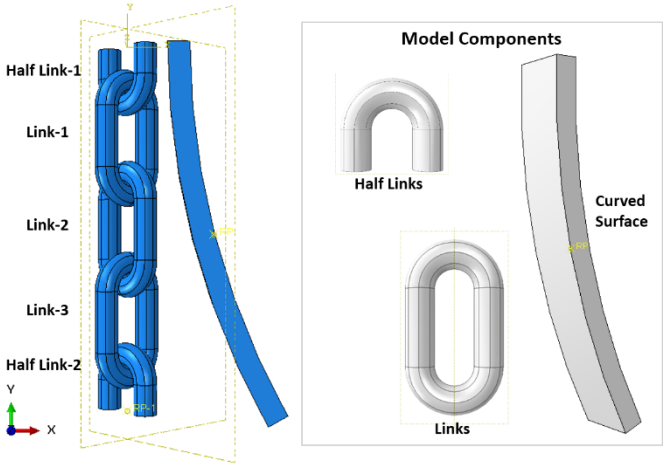
This article analyzes the influence of the interaction between mooring chain links and geometric barriers on the behavior of critical stress points, as well as the impact of the residual stress field on the obtained responses. The main objective of this research is to provide a basis for more accurate fatigue assessments that reflect the actual operating conditions of the mooring chain links.

2 Finite Element Modeling

In this section, we present the details of the finite element model of the chain links with a curved surface, developed using Abaqus/CAE software version 2019.

2.1 Problem modeling

The finite element model consists of the following components: a curved ungrooved surface, a chain composed of three complete links, and two half links. The half links are responsible for the beginning and end of the chain links assembly. Fig. 1 shows the assembly of the model, highlighting each of its constituent parts. Two reference points, RP and RP-1, were used to apply the load and boundary conditions.



a) Model assembly. b) Individual components.

Figure 1. Problem modeling details.

To reduce computational cost, the curved surface was modeled as a rigid body, and the analysis focused on the chain link set. To investigate the effects of varying the surface radius, five geometries with radii of 3535 mm, 4035 mm, 4535 mm, 5035 mm, and 5535 mm were considered. The links were designed according to normative guidelines, including fixed aspect ratios and dimensions dependent on the cross-sectional diameter [11]. A diameter of 105 mm was adopted.

After modeling the components and performing the assembly, contact conditions were defined between the interacting parts. A surface-to-surface contact formulation was adopted both for the interfaces between the links and for the contact between the links and the surface. The sliding formulation accounted for large displacements, and the discretization method adopted was also surface-to-surface. Contact properties considered hard contact in the normal direction and a frictional formulation with a coefficient of 0.3 in the tangential direction.

2.2 Material properties

The critical points are evaluated by considering elastoplastic material behavior, modeled by a Ramberg-Osgood law consistent with the quality of offshore steel grade R3, with the hardening behavior parameters adjusted to $K = 952$ and $n = 13.95$ [12]. The main material characteristics are presented in Tab. 1.

Table 1 - Properties of grade R3 offshore steel.

Mechanical properties	Symbol	Values
Young's Modulus	E [GPa]	210.0
Initial yield stress	σ_{y0} [MPa]	610.0
Ultimate stress	σ_u [MPa]	813.0 (true value)
Ultimate strain	ε_u [%]	11.33 (true value)
Poisson ratio	ν	0.3

2.3 Service loading and boundary conditions

The loading sequence applied to the model is defined in two phases: manufacturing and operation. In the manufacturing phase, the mooring is subjected to a proof load corresponding to 70% of the Minimum Breaking Load (MBL). According to Det Norske Veritas [11] and considering the model material properties, the proof load P_f (in kilinewtons) is expressed as a function of the link diameter d by

$$P_f = 0.0156d^2(44 - 0.08d). \tag{1}$$

In the operational phase, the applied load corresponds to a percentage of the MBL. This study investigates load levels of 20%, 40%, and 60% of MBL. Fig. 2 illustrates the loading sequence used during the simulation. Step 0-1 represents the application of the proof load, which is subsequently removed in step 1-2. In step 2-3 the operating load is gradually applied, and then kept constant in steps 3-4 and 4-5. Finally, a rotation is applied to the free end of the mooring chain links in the last step (4-5).

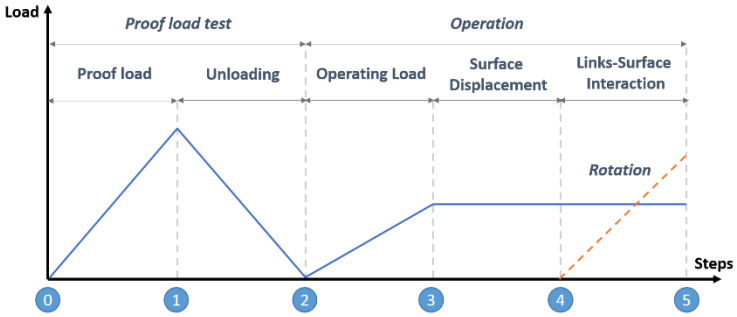
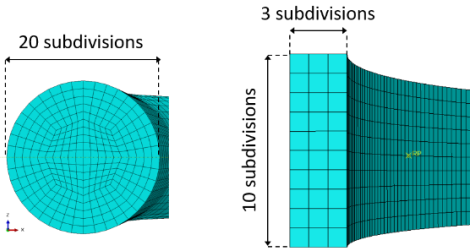


Figure 2. Load at each step.

Boundary conditions are constraints applied to the modeling to represent the expected behavior of the system. In the model studied in this article, five boundary conditions were applied, designated as BC-1, BC-2, BC-3, BC-4, and BC-5, each defined by properties: Displacement/Rotation condition applied to the fixed link in all loading steps, with displacement restricted along the X and Z axes (BC-1); Symmetry/Antisymmetry/Fixed condition also applied to the fixed link in all loading steps, with displacement restricted in the Y plane and rotations restricted in the X and Z planes (BC-2); Displacement/Rotation condition applied to the reference point (RP) of the curved surface illustrated in Fig. 1, with displacement along the X axis prescribed for initial contact with the links in the final step 3-4 (BC-3); Displacement/Rotation condition applied to the reference point (RP) of the curved surface illustrated in Fig. 1, with displacement restricted on the curved surface for all degrees of freedom during step 4-5 (BC-4); and Displacement/Rotation condition applied to the reference point (RP-1) of the mooring chain links illustrated in Fig. 1, with a prescribed rotation about the Z axis in step 4-5 (BC-5).

2.4 Finite element mesh

The element type selected for the set of links is C3D8I, an eight-node hexahedral finite element enriched with incompatible modes. For the curved surface, the quadrilateral rigid element R3D4 was adopted. Details of this discretization are shown in Fig. 3. The mesh convergence test showed that further refinement led to a difference of about 1% in the maximum principal stress, at the expense of a high computational cost. Therefore, the adopted discretization was considered adequate for the analysis.



a) Link. b) Curved surface.

Figure 3. Finite element mesh details.

3 Stress Concentration Factors

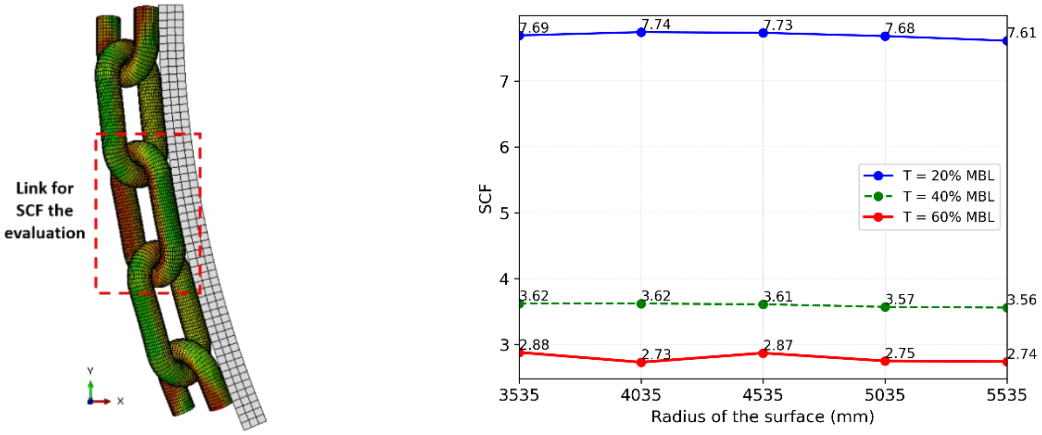
The basic stress formulas used in structural member design are derived under the assumption that the members possess a constant section or a section with gradual change of contour. However, the presence of geometric discontinuities results in modifications of stress distributions. At these points, the stress locally increases relative to the nominal stress. This localization is known as the critical stress point, quantified by the Stress Concentration Factor (SCF). The SCF, denoted by K_t, is defined as the ratio between the maximum stress σ_{max} expected in the member and a reference stress σ_{nom} [13]:

$$K_t = \frac{\sigma_{max}}{\sigma_{nom}}, \tag{2}$$

The effect of stress concentration is crucial in understanding many failure mechanisms, especially fatigue cracking [14]. The initiation of fatigue cracks is governed by the history of stress or strain ranges and by the occurrence of maximum stress peaks at the critical point [15].

4 Results and discussion

A total of 15 numerical models were used to evaluate the influence of geometric barriers on the SCFs of the mooring chain links. The results presented in this section refer specifically to Link-2. Fig. 4 illustrates the deformed configuration of the model in the final loading step, and the SCFs obtained for the case with a curved surface.



a) Final-step deformed model configuration. b) SCFs under varying surface radii and operating loads.

Figure 4. Evaluation of the interaction effect between geometric barriers and mooring chain links.

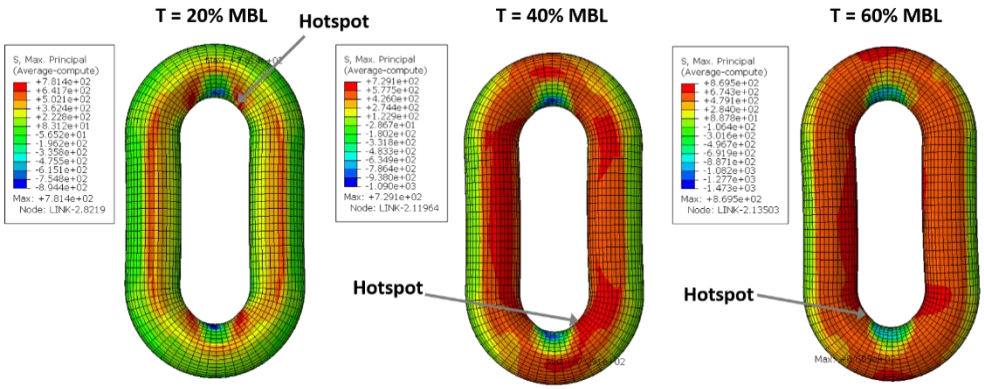
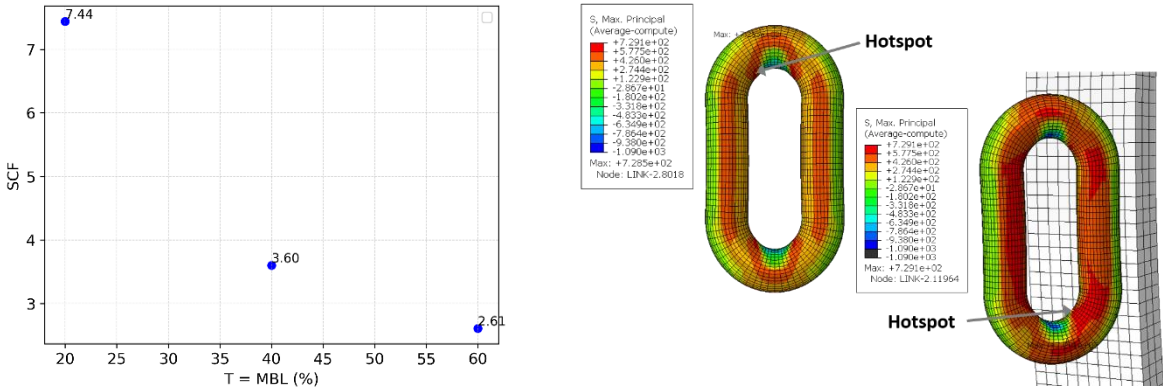


Figure 5. Hotspots localization with the presence of a curved surface.

Considering operating loads of 20%, 40%, and 60% of the MBL, the average SCF values are 7.69, 3.60, and 2.79, respectively. It can be observed that the SCFs vary significantly with changes in the operating load, and that the hotspot location is also altered. Fig. 5 indicates the hotspot location for the three operating load percentages investigated, considering the interaction between the links and a surface with a radius of 4535 mm. All critical points presented are located on the free surface.

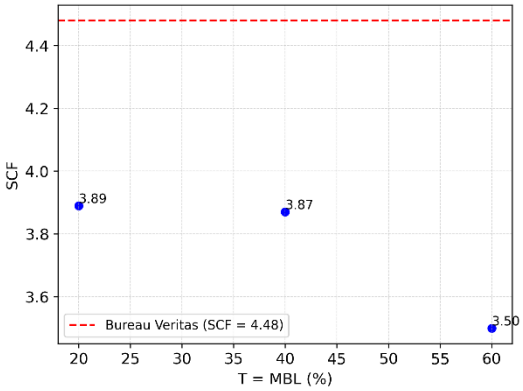
Furthermore, when evaluating the critical stress points without the presence of the geometric barriers, the SCFs obtained were 7.44 at 20% of the MBL, 3.60 for 40% of the MBL, and 2.61 for 60% of the MBL, as shown in Fig. 6(a). Compared to the average values presented previously, a small variation in the SCF values is observed. However, it was observed that both the stress distribution and the critical point location change. Fig. 6(b) presents the stress distribution and the localization of the hotspot for the condition with and without the geometric barrier, considering an operating load of 40% of the MBL and surface with a radius of 4535 mm.



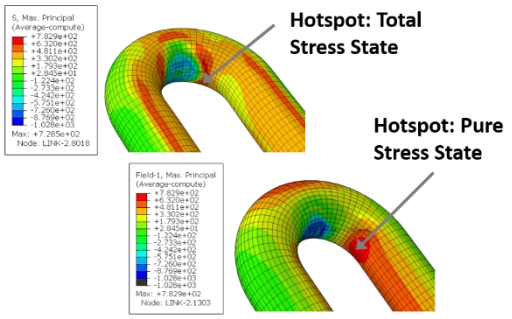
a) SCFs without the presence of the geometric barriers. b) Stress distribution and hotspot localization.

Figure 6. Analysis of critical points without the presence of the geometric barriers.

Typically, SCFs of mooring chain links are determined from stress states generated for specific loading modes, in which a pure stress state is sought. In this case, pre-existing residual stresses in the links are omitted. For the tension loading condition, for example, Bureau Veritas recommends an SCF of 4.48 in such a situation [3]. Fig. 7(a) presents the SCFs results obtained considering the pure stress state of the operating load. Comparing the results presented in Fig. 7(a) with those in Fig. 6(a), it was observed that residual stresses have a substantial impact on the SCFs results. Furthermore, notable changes were detected in the stress distribution along the chain link and in the location of the hotspot. Fig. 7(b) illustrates these results for an operating load of 40% of the MBL, without interaction of the chain links with the surface.



a) SCFs for pure stress state without curved surface.



b) Stress distribution and hotspot localization.

Figure 7. Effect of evaluating the results considering the pure stress state.

Fatigue analyses for tie links typically use the S-N curve, which assumes linear behavior between stress and strain. This approach aligns with the phenomenon known as *Elastic Shakedown*, observed when the test load applied to the links causes the material to work harden, causing it to behave in a linearly elastic manner after unloading, without accumulating additional plastic strain.

In this study, the presence of additional plastic strain at the end of each loading step was investigated. The analysis, conducted for different levels of operational tension, indicated that, at the end of the operating load application step, the maximum accumulated plastic strain was the same as that obtained at the end of the test load step. In other words, no increase in plastic strain during operating loading, with the maximum accumulated plastic strain value being 0.157.

When considering the interaction between the links and the curved surface with radius 4535 mm, the evaluation of the additional plastic strain in the last loading step showed that, for operating load corresponding to 20% of the MBL, the plastic strain value remained constant at 0.157. However, for 40% of the MBL, the maximum accumulated plastic strain increased to 0.166, and, for 60% of the MBL, this value reached 0.287. Variation in the radius of the curved surface also influenced the accumulated plastic strain. Fig. 8 shows the results obtained for an operating load of 60% of the MBL, considering the interaction between the links and surfaces with radii of 4035, 4535, and 5035 mm.

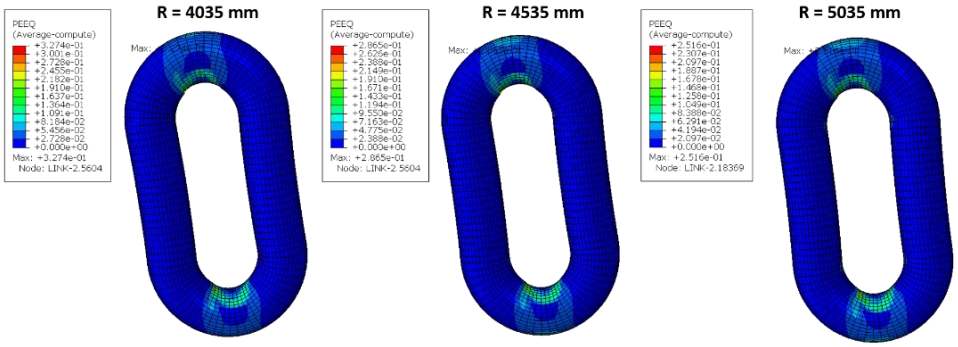


Figure 8. Accumulated plastic strain for an operating load of 60% of the MBL and different surface radii.

Fatigue assessment of mooring chain links is often carried out under the assumption of linear behavior. These approaches rely on high-cycle fatigue, where stresses are small relative to the yield strength and failure occurs only after a large number of cycles. In contrast, nonlinear fatigue methodologies should be addressed within the low-cycle fatigue regime, where the elastoplastic strain history is significant.

5 Conclusions

Evaluation of the interaction between mooring chain links and geometric barriers shows that changes in the operating load significantly affect the SCFs and the location of the critical stress points. This behavior suggests that the nonlinearity of the problem does not ensure that these factors remain constant when certain input parameters of the numerical model are modified. Changes in other parameters, such as the link diameter, are also expected to affect the results.

Investigating the problem in the absence of the geometric barrier, the interaction between the links and the curved surface does not significantly affect the SCF values, showing only small variations around the mean value obtained with the geometric barrier. On the other hand, the stress distribution along the link and the location of the critical stress point are altered. Furthermore, comparison of the total stress state of the links with the pure stress state of the operating load reveals that the stress distribution, the SCFs, and consequently the location of the critical stress points are significantly modified. This outcome can directly impact the fatigue life of the mooring chain links.

When evaluating the accumulated plastic strain throughout the loading steps, the results suggest that fatigue assessments based solely on linear relationships may underestimate the actual damage to the links, indicating that methodologies that account for nonlinear effects are more appropriate for the presented problem. All results presented in this article are intended to contribute to more accurate and representative fatigue assessments of mooring chain links under real operating conditions.

Acknowledgements. The authors acknowledge PETROBRAS and CNPq for the financial support.

Authorship statement. The authors hereby confirm that they are the sole liable persons responsible for the authorship of this work, and that all material that has been herein included as part of the present paper is either the property (and authorship) of the authors, or has the permission of the owners to be included here.

References

[1] E. Fontaine, A. Kilner, C. Carra, D. Washington, K. T. Ma, A. Phadke, D. Laskowshi and G. Kusinski, “Industry survey of past failures, pre-emptive replacements and reported degradations for mooring systems of floating production units”. In: *Offshore Technology Conference. Houston (OTC)*, p. OTC–25273-MS, 2014.
[2] X. Xue. Fracture Mechanics Based Offshore Mooring Fatigue Assessment. PhD thesis, Newcastle University, 2019.
[3] Bureau Veritas, “Fatigue of Top Chain of Mooring Lines due to In-plane and Out-of-plane Bending: Guidance Note NI 604 DT R00E”. Bureau Veritas, 2014.
[4] American Bureau of Shipping, “Guide for Position Mooring Systems”, American Bureau of Shipping, 2022.
[5] American Petroleum Institute, “API RP 2SK: design and analysis of stationkeeping systems for floating structures”, American Petroleum Institute, 2024.
[6] M. Luo and C. Heyl, “Numerical study on the out-of-plane bending (OPB) behaviors of studless mooring chain links in fairlead structures”. In: Proceedings of the Twenty-seventh, *International Ocean and Polar Engineering Conference (ISOPE)*, pp. 1106-1112, 2017.
[7] M. Z. Silva. Study on the Influence of Wear on the Premature Failure of Mooring Line Components. Master's thesis, University of Brasília, 2017.
[8] X. Xue, N-Z Chen, Y. Pu, L. Chen and L. Wang. “Fracture mechanics assessment for mooring chain links tensioned over a curved surface”. *Applied Ocean Research*, vol. 117, pp. 102900, 2021.
[9] P. M. C. L. Pacheco, M. A. Savi, P. P. Kenedi, J. C. F. Jorge and H. G. Santos, “Finite element residual stress analysis applied to offshore studless chain links”. In: 23rd *International Conference on Offshore Mechanics and Arctic Engineering (OMAE)*, 2004.
[10] J. Choung and J. Lee, “Study on prediction of stresses by out-of-plane and in-plane bending moments in offshore mooring chain”. *Ships and Offshore Structures*, vol. 13, 2018.
[11] Det Norske Veritas, “DNVGL-OS-E302, Offshore standard – offshore mooring chain”, DNV, 2018.
[12] L. Rampi. RR-M-86-007 Chain Out of Plane Bending - JIP Report. 2013. Unpublished report.
[13] W. D. Pilkey. *Peterson’s stress concentration factors.* John Wiley & Sons, 1997.
[14] J. T. P. de Castro and M. A. Meggiolaro. *Fatigue Design Techniques: Under Real Service Loads*. Createspace Independent Publishing Platform, vol. 1, 2016.
[15] A. C. O. Miranda, M. A. Antunes, M. V. G. Alarcón, M. A. Meggiolaro and J. J. T. P. de Castro, “Use of the stress gradient factor to estimate fatigue stress concentration factors K_f”. *Engineering Fracture Mechanics*, vol. 206, pp. 250-266, 2019.